

Topology in Physics: Some recent applications

Calum Ross¹,
September 2020

Contents

1	Introduction	1
2	A primer on solitons	1
2.1	What is a topological soliton	1
2.2	Examples of solitons	2
2.3	Derrick's Theorem and solitons in higher dimensions	7
2.4	Stability of one dimensional solitons	8
2.5	Topological degree	9
2.6	Higher dimensional examples	10
3	Solitons in chiral magnets	11
3.1	The $O(3)$ sigma model	11
3.2	Derrick's Theorem for chiral magnets	13
3.3	Magnetic Skyrmions model	14
3.3.1	The vacuum manifold	14
3.3.2	Hedgehogs and symmetries of the model	16
3.4	The solvable line	17
3.5	The critically coupled model	19
3.5.1	A zoo of skyrmions	22
3.6	A comment on boundary terms	27
3.7	A view to the future	28

1 Introduction

These notes are to complement two lectures that I gave on topological solitons as part of an LMS scheme 3 grant to NBMPS. The material in these notes has more detail and extends the content of the lectures. The main references for background material on topological solitons are [MS04] and [Col88]. For magnetic skyrmions the main reference is [BSRS20]. I have included some exercises in red that are worth solving if you want to fully understand the material.

2 A primer on solitons

2.1 What is a topological soliton

The first thing that we need to establish is what exactly is a topological soliton in a field theory. A great resource for this material and the inspiration for a lot of this section is Chapter 6 in

¹If there are any comments or corrections that you feel I should know about you can contact me at c.ross[at]keio.jp

[Col88]. In most field theories the finite energy, non-singular, solutions are dissipative and they eventually decay to the vacuum. However, there are examples of field theories with static solutions that are lumps of energy which hold themselves together through self-interaction. There can be more complicated non-dissipative solutions which are periodic in time or have a complicated time-dependence. If the theory is Lorentz or Galilean invariant then static lumps can be boosted to give time-dependent solutions.

There are two useful definitions of a soliton:

1. (weak) The lump of energy does not dissipate, it can propagate and it has finite energy.
2. (strong) The lumps satisfy the weak definition and survive scattering with other lumps.

In [Col88] solitons are called lumps with soliton reserved for lumps which satisfy the strong definition. The topology comes in from the space of finite energy, non-singular, field configurations. We say that a soliton is topological if it can not be continuously deformed to the vacuum through a path in the space of finite energy, non-singular, field configurations. In these notes we will be quite cavalier with the term topological.

2.2 Examples of solitons

The most common examples of field theories possessing topological soliton solutions are ϕ^4 model and the Sine-Gordon model both considered in $1+1$ dimensions. As these theories only differ in the choice of potential term we first set out some general conventions about $1+1D$ scalar field theories. We work with the metric such that $g_{00} = 1 = -g_{11}$ and consider the Lagrangian density,

$$\mathcal{L} = \frac{1}{2} \partial_\mu \phi \partial^\mu \phi - U(\phi), \quad (2.1)$$

and energy

$$E = \int dx \left[\frac{1}{2} (\partial_0 \phi)^2 + \frac{1}{2} (\partial_1 \phi)^2 + U(\phi) \right]. \quad (2.2)$$

It is sometime convenient to split off the kinetic and potential energy terms as

$$T = \int dx \left[\frac{1}{2} (\partial_0 \phi)^2 \right], \quad (2.3)$$

$$V = \int dx \left[\frac{1}{2} (\partial_1 \phi)^2 + U(\phi) \right]. \quad (2.4)$$

The equation of motion following from Eq. (2.1) is

$$\partial_\mu \partial^\mu \phi + \frac{dU(\phi)}{d\phi} = 0. \quad (2.5)$$

We assume that the energy is bounded below a minimum value which implies that $U(\phi)$ is bounded below² by some constant, U_0 . It follows from Eq. (2.2) that a state of minimum energy, called a ground state or vacuum, is a field ϕ_0 such that

$$\partial_1 \phi_0 = \partial_0 \phi_0 = 0, \quad U(\phi_0) = U_0. \quad (2.6)$$

²It is conventional to assume that $U_0 = 0$ so that $E \geq 0$. If $U_0 \neq 0$ we can just add the constant U_0 to Eq. (2.2) so that $E \geq 0$.

That is a ground state is a field configuration that is static, spatially constant, and a minimum of the potential. The set of such ground states is sometimes called the vacuum manifold

$$\mathcal{V} = \{\phi \mid U(\phi) = 0\}. \quad (2.7)$$

We are now ready to treat the two examples.

1. ϕ^4 : In the ϕ^4 model the potential is taken to be

$$U(\phi) = \frac{\lambda}{2} (\phi^2 - a^2)^2 \quad (2.8)$$

with λ the positive coupling constant and a related to the conventional mass parameter μ through $a^2 = \frac{\mu^2}{\lambda}$, and $\phi : \mathbb{R} \rightarrow \mathbb{R}$ a real scalar field. This potential has two zeros at $\phi = \pm a$ as can be seen in Fig. 1. Another way to say this is that the vacuum manifold is

$$\mathcal{V} = \{-a, a\}. \quad (2.9)$$

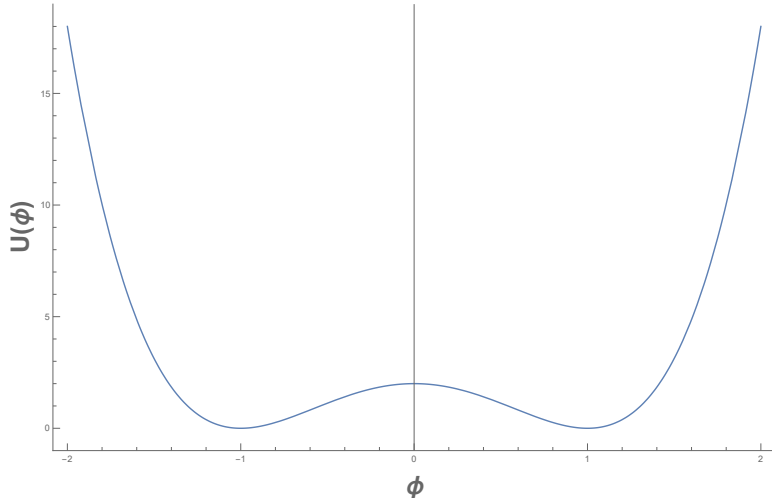


Figure 1: A plot of the potential term in the ϕ^4 model, Eq. (2.8) for $a = 1, \lambda = 4$.

2. Sine-Gordon: The potential term for the Sine-Gordon model is

$$U(\phi) = \frac{\alpha}{\beta^2} (1 - \cos(\beta\phi)) \quad (2.10)$$

with $\alpha, \beta \in \mathbb{R}$ and $\beta > 0$. The \cos term is $\frac{2\pi}{\beta}$ periodic so the vacuum manifold is

$$\mathcal{V} = \{\phi = \frac{2\pi}{\beta}k \mid k \in \mathbb{Z}\}. \quad (2.11)$$

The Sine-Gordon potential is plotted in Fig. 2. Focusing on the ground state at $\phi = 0$ and expanding the potential around it we find

$$U(\phi)|_{\phi=0} \simeq \frac{\alpha}{2}\phi^2 - \frac{\alpha\beta^2}{4!}\phi^4 + \dots \quad (2.12)$$

which looks like a ϕ^4 term with $\lambda \sim \alpha\beta^2$ and $\mu^2 \sim \alpha$.

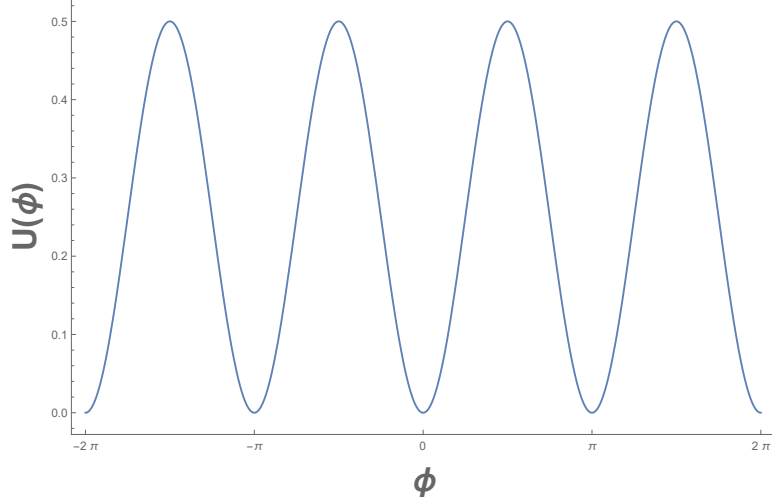


Figure 2: A plot of the potential term in the Sine-Gordon model, Eq. (2.10) for $\alpha = 1, \beta = 2$.

To find static solutions³ in either model we consider

$$\delta V = \delta \int dx \left[\frac{1}{2} (\partial_1 \phi)^2 + U(\phi) \right] = 0, \quad (2.13)$$

subject to

$$\lim_{x \rightarrow \pm\infty} \phi(x) \in \mathcal{V}. \quad (2.14)$$

The condition that ϕ tends to the vacuum manifold asymptotically is there to ensure that the solution has finite energy.

First we note that if \mathcal{V} is just a point, there is only one ground state, then the only solution is the constant ground state.

If \mathcal{V} has more elements then there exist non-trivial static solutions interpolating between neighbouring elements of \mathcal{V} . Spelling this out in more detail there are solutions $\phi(x)$ which are monotonic from $\phi(-\infty) = \phi_-$ to $\phi(\infty) = \phi_+$ for

$$\mathcal{V} = \{\dots, \phi_-, \phi_+, \dots\}. \quad (2.15)$$

In [Col88] there is a nice analogy between the field theory and the motion of a particle in one dimension subject to a potential with multiple minima.

If ϕ is monotonically increasing, $\phi_- < \phi_+$ then the solution is a soliton. While if ϕ is monotonically decreasing, $\phi_- > \phi_+$ then the solution is an antisoliton.

Before we start to construct explicit soliton configurations it is a good time to stop and check where the topology comes in to this. There is a correspondence between the boundary data and the solution, that is $(\phi_+, \phi_-) \in \mathcal{V} \times \mathcal{V}$ classifies the configuration. When $\phi_+ = \phi_-$ the configuration can be continuously deformed to the ground state ϕ_+ , while for $\phi_+ \neq \phi_-$ the configuration ϕ cannot be deformed to a ground state configuration in \mathcal{V} . This is because

³That is solutions such that $\partial_0 \phi = 0$.

the space of non-singular field configurations has several disconnected components labelled by $\phi_+ \times \phi_-$.

Example 2.1. Consider ϕ^4 theory. $\mathcal{V} = \{-a, a\}$ so the possible boundary configurations are $(-a, -a)$, $(-a, a)$, (a, a) , $(a, -a)$. These are the four connected components of the space of finite energy field configurations.

- $(-a, -a)$ is equivalent to the constant $\phi = -a$.
- $(-a, a)$ the field configuration is a soliton.
- $(a, -a)$ the field configuration is an antisoliton.
- (a, a) is equivalent to the constant $\phi = a$.

We distinguish between the configurations using the integer

$$N = \frac{1}{2a} \int_{-\infty}^{\infty} dx \frac{d\phi}{dx} = \frac{\phi_+ - \phi_-}{2a} \in \mathbb{Z} \quad (2.16)$$

known as the topological charge as it tells us which connected component the field configuration is in.

We can generalise this analysis to see that the asymptotic data (ϕ_+, ϕ_-) labels the connected component of the space of finite energy field configurations that we are considering. The topology of the soliton comes from the topology of the vacuum manifold⁴ through $\pi_0(\mathcal{V})$.

Exercise 2.2. Consider the Sine-Gordon model, what are the connected components of \mathcal{V} ? Knowing the connected components how can we assign an integer to the field configurations?

Considering the static energy Eq. (2.4) it is a straightforward completing the square computation to see that

$$E = \int_{-\infty}^{\infty} dx \left[\frac{1}{2} \left(\partial_1 \phi \mp \sqrt{2U(\phi)} \right)^2 \pm \sqrt{2U(\phi)} \frac{d\phi}{dx} \right] \geq \left| \int_{\phi_-}^{\phi_+} d\phi \sqrt{2U(\phi)} \right|. \quad (2.17)$$

To justify this bound it is instructive to expand the squared term,

$$\begin{aligned} \frac{1}{2} \left(\partial_1 \phi \mp \sqrt{2U(\phi)} \right)^2 &= \frac{1}{2} \left[(\partial_1 \phi)^2 \mp 2\partial_1 \phi \sqrt{2U(\phi)} + 2U(\phi) \right], \\ &= \frac{1}{2} (\partial_1 \phi)^2 + U(\phi) \mp \frac{d\phi}{dx} \sqrt{2U(\phi)}. \end{aligned} \quad (2.18)$$

This is $1+1D$ energy density from Eq. (2.2) with the addition of $\mp \frac{d\phi}{dx} \sqrt{2U(\phi)}$, the negative of the term added in Eq. (2.17). If $U(\phi)$ is bounded then we can find a “superpotential” $W(\phi)$ such that

$$U(\phi) = \frac{1}{2} \left(\frac{dW}{d\phi} \right)^2 \quad (2.19)$$

⁴The space of finite energy, non-singular field configurations, often called the configuration space \mathcal{C} , also has non-trivial topology as it is not connected. As was said above these configurations are classified by their asymptotic values, which are in \mathcal{V} , which is why we focus on the topology of \mathcal{V} .

and the bound, known as the Bogomol'nyi bound, becomes

$$E \geq |W(\phi_+) - W(\phi_-)|. \quad (2.20)$$

As we are interested in the minima, at least the minima within a given topological sector, we want to construct configurations which saturate this Bogomol'nyi bound. Thus we do not need to solve the full second order equations of motion, Eq. (2.5), but can solve the first order Bogomol'nyi equations

$$\partial_1 \phi \mp \sqrt{2U(\phi)} = 0, \quad (2.21)$$

which imply the second order equations of motion.

These Bogomol'nyi equations can be solved by quadratures to find

$$x - x_0 = \pm \int_{\phi_0}^{\phi} \frac{d\varphi}{\sqrt{2U(\varphi)}}, \quad (2.22)$$

where x_0 is the centre of the soliton such that $\phi(x_0) = \phi_0$ is an arbitrary point between ϕ_- and ϕ_+ .

Example 2.3. Considering the ϕ^4 model the potential is given by (2.8). Choosing the asymptotics $\phi_{\pm} = \pm a$ enables us to write Eq. (2.22) as

$$x = \pm \frac{1}{\mu} \int_0^{\phi} \frac{d\varphi}{\frac{\varphi^2}{a^2} - 1} = \mp \frac{1}{\mu} \operatorname{arctanh} \left(\frac{\phi}{a} \right). \quad (2.23)$$

Inverting this we have that the ϕ^4 kink is

$$\phi(x) = a \tanh (\mu x), \quad (2.24)$$

taking the negative sign gives the anti-kink. The ϕ^4 kink solution is plotted in Fig. 3.

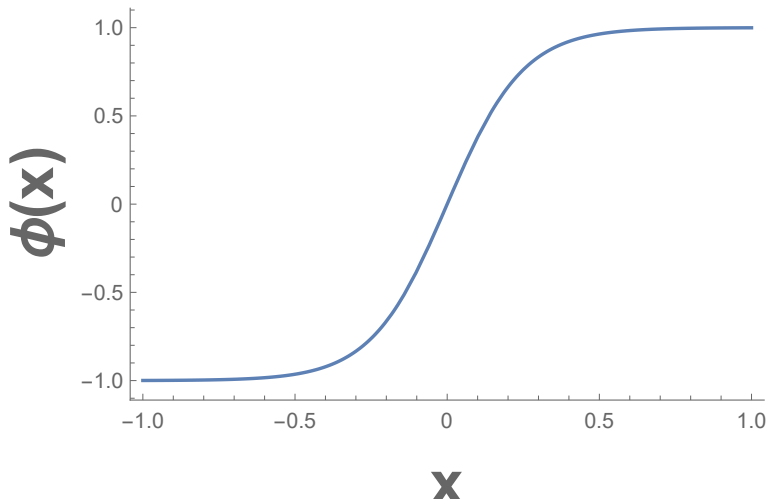


Figure 3: A plot of the kink solution in the ϕ^4 model, Eq. (2.24) for $a = 1, \mu = 4$.

Exercise 2.4. Working with the static energy for the Sine-Gordon model solve the Bogomol'nyi equations to show that the Sine-Gordon kink is given by

$$\phi(x) = \frac{4}{\beta} \arctan(\exp(\sqrt{\alpha}x)). \quad (2.25)$$

Next show that the energy of the kink is

$$E|_{\text{kink}} = \frac{8\sqrt{\alpha}}{\beta^2}. \quad (2.26)$$

The Sine-Gordon kink is plotted in Fig. 4

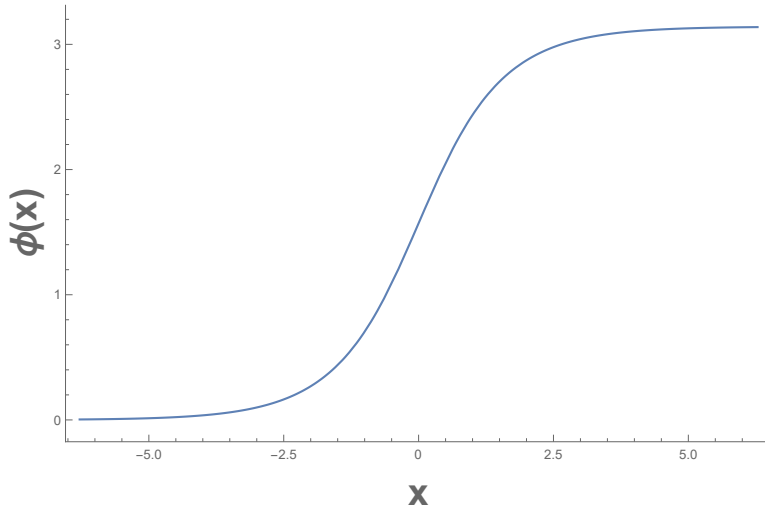


Figure 4: A plot of the kink solution in the Sine-Gordon model, Eq. (2.25) for $\alpha = 1, \beta = 2$.

2.3 Derrick's Theorem and solitons in higher dimensions

For theories in spatial dimensions greater than one it is more complicated to construct static soliton solutions. This is in part because of the following Theorem.

Theorem 2.5 (Derrick's Theorem [Der64]). *Consider a vector, ϕ , constructed from n -scalar fields in $1+D$ dimensions,*

$$\phi : M^{1+D} \rightarrow N^n. \quad (2.27)$$

Assume that the dynamics of the fields is governed by

$$\mathcal{L} = \frac{1}{2} \partial_\mu \phi \cdot \partial^\mu \phi - U(\phi), \quad (2.28)$$

with U non-negative and bounded below⁵. Then for $D > 2$ the only non-singular, finite energy, static solutions are elements of \mathcal{V} , the ground states.

⁵We saw above that as long as U is bounded we can always add a constant so that it is non-negative

This is proved using a scaling argument.

Proof. Define

$$V_1 = \frac{1}{2} \int d^D x (\nabla \phi)^2, \quad (2.29)$$

$$V_2 = \int d^D x U(\phi). \quad (2.30)$$

The V_i are non-negative and bounded below by zero. Next given a static solution $\phi(x)$ we can define the scaled solution

$$\phi_\lambda(\vec{x}) \equiv \phi(\lambda \vec{x}), \quad \lambda \in \mathbb{R}_+. \quad (2.31)$$

The potential energy of the scaled solution is

$$V_\lambda = \lambda^{2-D} V_1 + \lambda^{-D} V_2. \quad (2.32)$$

By assumption $\phi(x)$ is a minimum of the energy, thus it is a minimum with respect to scaling:

$$\left. \frac{dV_\lambda}{d\lambda} \right|_{\lambda=1} = -[(D-2)V_1 + D V_2] \stackrel{!}{=} 0. \quad (2.33)$$

Unpacking this statement we have that for $D > 2$, as the V_i are bounded below by zero, the solution is $V_1 = V_2 = 0$. \square

We can also say something when $D = 2$. The same logic as above implies that $V_2 = 0$. However, V_1 is now scale invariant so non-trivial scale invariant solutions, such as the lumps in the $O(3)$ sigma model that we will meet later, are possible.

Another way to state the proof of Derrick's Theorem is that the scaled potential, V_λ is monotonically decreasing as λ increases and thus has no stationary points.

There are several ways to circumvent Derrick's theorem they include: Adding higher order terms to the energy functional, such as the skyrme term in two and three dimensions. Adding a term which is not bounded below, such as the Dyaloshinskii-Moriya term that we will encounter later. Explicitly constructing time dependent solutions. Finally coupling to a gauge field gives another means of subverting the assumptions of the theorem. Many of the most famous examples of topological solitons are obtained in gauge theories. These include, vortices, magnetic monopoles, and instantons.

2.4 Stability of one dimensional solitons

When we constructed our soliton solutions in the ϕ^4 and Sine-Gordon models, Eqs. (2.24) and (2.25) we did not show that they were stable with respect to small perturbations. This is again a topic that is treated in detail in [Col88]. The equation of motion coming from the Lagrange density in Eq. (2.1) is

$$\square^2 \phi + \frac{dU(\phi)}{d\phi} = 0 \quad (2.34)$$

as we saw in Eq. (2.5). Consider a field configuration which includes fluctuations, $\delta(x, t)$, around a static solution⁶, $f(x)$, of the equations of motion

$$\phi(x, t) = f(x) + \delta(x, t), \quad (2.35)$$

inserting this into Eq. (2.34) and working to linear order in δ we find

$$\square^2 \delta(x, t) + \frac{d^2 U(f)}{dx^2} \delta = 0. \quad (2.36)$$

As this equation is invariant under time translations a solution can be written as a sum of normal modes in the following way

$$\delta(x, t) = \Re \left[\sum_n a_n e^{i\omega_n t} \psi_n(x) \right], \quad (2.37)$$

where \Re means taking the real part, the a 's are the arbitrary complex coefficients, and ω_n, ψ_n solve the Schrödinger equation

$$-\frac{d^2 \psi_n}{dx^2} + \frac{d^2 U(f)}{dx^2} \psi_n = \omega_n^2 \psi_n. \quad (2.38)$$

The solutions are stable if and only if the eigenvalues are all positive, $\omega_n^2 \geq 0 \forall n$. We now demonstrate that this is the case. The easiest solution to Eq. (2.38) is $\psi_0 = \frac{df}{dx}$ with eigenvalue $\omega_0 = 0$. Now since f is monotone the function ψ_0 has no nodes. Finally we just need to use the well known result that for a one-dimensional Schrödinger equation with an arbitrary potential the lowest energy eigenfunction is the one with no nodes [MF53]. This means that ψ_0 is the lowest energy solution of Eq. (2.38) and thus $\omega_n \geq 0 \forall n$ as we required.

In the language of quantum mechanics we have expanded in quantum fluctuations around the background of the soliton. The existence of classical solutions which are not in \mathcal{V} leads to interesting and non-trivial backgrounds to do quantum mechanics around.

Exercise 2.6. Considering the Sine-Gordon model with soliton solution given in Eq. (2.25) construct the Schrödinger equation of Eq. (2.38). First find the zero-mode, ψ_0 with eigenvalue zero, then construct the continuum of scattering states with $\omega_n^2 > 0$.

2.5 Topological degree

This section is just a brief summary of some of the key ideas, for more detail I refer the readers to [MS04, Dun10]. The particular expressions for the topological charge that I use will be introduced when they are needed.

We have seen a quantity called the topological charge show up in both the ϕ^4 and the Sine-Gordon model. In these one dimensional models the topology was due to the connected components of \mathcal{V} , given by $\pi_0(\mathcal{V})$.

⁶Even though we are perturbing around a static solution we consider time dependent perturbations.

In higher dimensions the topology arises from the higher homotopy groups of \mathcal{V} , the target space, or in the case of gauge theories from the Chern numbers of the gauge bundle. The full story is explained in [MS04] and [Dun10] and I will only discuss the degree expressions that I need to use.

The basic story is that a field configuration can be viewed as a map between the domain, X , and the target space⁷ Y , with $\dim X = \dim Y$. Now a map $\phi : X \rightarrow Y$ between topological spaces lifts to a map of cohomology groups⁸ [Hat00]

$$\phi^* : H^i(Y) \rightarrow H^i(X). \quad (2.39)$$

The degree is then defined in terms of a normalised⁹ volume form Ω_Y on Y as

$$\deg\phi = \int_X \phi^*(\Omega_Y) \in \mathbb{Z}. \quad (2.40)$$

I do not prove here that the degree is an integer but the proof is given in both [MS04] and [Dun10].

The most common examples are when $\phi : S^n \rightarrow S^n$, in this setting the degree is often called the winding number.

Example 2.7. A good example to have in mind, taken straight from [MS04], is when $X \simeq Y \simeq S^1$. The normalised volume form on S^1 is $\Omega_{S^1} = \frac{1}{2\pi} d\theta$ and Eq. (2.40) reduces to

$$\deg\phi = \frac{1}{2\pi} \int_0^{2\pi} \frac{d\phi}{d\theta} d\theta = \frac{1}{2\pi} (\phi(2\pi) - \phi(0)), \quad (2.41)$$

which is a measure of how many times ϕ goes around the target circle while going around the domain once.

Another way to compute the degree is in terms of a signed count of the preimages of a regular value, again we refer to [MS04] for the details.

2.6 Higher dimensional examples

Before moving on to the specific examples that we want to study in detail let us take the opportunity to showcase several examples of topological solitons in dimension two and three.

1. On \mathbb{R}^2 consider $U(1)$ gauge theory with a single complex scalar field¹⁰ The potential is taken to be

$$U(\phi) = \frac{\lambda}{2} (|\phi|^2 - a^2)^2 \quad (2.42)$$

⁷We also need both the domain and the target to be compact so that the integral of the volume form is well defined.

⁸Readers familiar with the concept of topological degree will notice that I am being rather relaxed in my discussion of it. For one thing it can be defined in terms of the lift of ϕ to a map of homotopy groups, however, this definition is less useful for computations so I focus on the cohomological interpretation.

⁹Normalised here means that $\int_Y \Omega_Y = 1$ so we are restricted to finite volume manifolds such as spheres. The conventional setting is that of closed manifolds and proper maps as explained in [MS04].

¹⁰This theory is sometimes called scalar QED and sometimes called the Abelian-Higgs model.

resulting in the vacuum manifold being

$$\mathcal{V} = \{\phi = ae^{i\sigma} | \sigma \in \mathbb{R}\} \simeq S^1. \quad (2.43)$$

In this case the topology arises from the space of maps $S^1 \rightarrow S^1$ with $\pi_1(S^1) = \mathbb{Z}$. The S^1 on the left is the boundary circle of infinite radius within \mathbb{R}^2 . The winding number is computed from

$$n = \int_0^{2\pi} \frac{d\sigma}{2\pi} = \int_0^{2\pi} \frac{d\theta}{2\pi} \frac{d\sigma}{d\theta} = \frac{1}{2\pi} \oint d\ln \phi. \quad (2.44)$$

This gives a model of the vortices in type II superconductors with the magnetic flux related to the winding number as $\Phi = \frac{2\pi n}{e}$.

2. The next example is on \mathbb{R}^3 with ϕ an isotensor, a real 3×3 symmetric matrix. We will not give the explicit expression for $U(\phi)$ but will assume that the vacuum manifold has the form¹¹

$$\mathcal{V} = \{\phi = 2aee^T - a(\mathbb{I} - ee^T) | a \in \mathbb{R}, e^2 = 1\}. \quad (2.45)$$

Here e is a real eigenvector of ϕ with eigenvalue $2a$. The other two eigenvalues of ϕ will be orthogonal to e with eigenvalue $-a$. As $e \in S^2$ and e and $-e$ have the same eigenvalue the vacuum manifold from Eq. (2.45) is the real projective plane

$$\mathcal{V} \simeq \mathbb{RP}^2. \quad (2.46)$$

The relevant homotopy group is $\pi_1(\mathbb{RP}^2) = \mathbb{Z}_2$ which leads to configurations with non-trivial topology.

Several other examples of models with and without topology are given in [Col88]. At this point it is worth noting what happens when we are considering a gauge theory, such as in the first example above, this involves a brief discussion of spontaneous symmetry breaking. Up to a gauge transformation the ground states are configurations where the gauge field vanishes and the scalar field is a constant such that $U = 0$. For a ground state, $\phi = \phi_0$, the unbroken part of the gauge group is $H \subset G$ such that $h\phi_0 = \phi_0 \forall h \in H$. As the potential U is G invariant when ϕ_0 is a zero of the potential $g\phi_0$ will also be a zero $\forall g \in G$. If we assume that all zeros of U can be written in this way, see [Col88] for a justification, then the vacuum manifold is isomorphic to G/H .

Exercise 2.8. Considering the two examples above what are the groups G and H ?

3 Solitons in chiral magnets

3.1 The $O(3)$ sigma model

The next type of topological solitons that we encounter are solitons in chiral magnets. Chiral magnets are described by an energy functional which is a version of a non-linear sigma model.

¹¹Such a potential will be expressible as $U(\phi) = \alpha \text{tr}(\phi^2) + \beta \text{tr}(\phi^3) + \gamma \text{tr}(\phi^4)$.

Here we focus on the static energy of the models and hold off on any discussions about time dependence. The field in the model is the magnetisation vector field of a magnetic material, $m : \mathbb{R}^2 \rightarrow S^2$, in other words m is a normalised three component vector. The energy functional consists of three pieces¹², the Dirichlet term

$$E_D[m] = \frac{1}{2} \int_{\mathbb{R}^2} d^2x (\nabla m)^2, \quad (3.1)$$

the potential term

$$E_{\text{potential}}[m] = \int_{\mathbb{R}^2} d^2x U(m), \quad (3.2)$$

and the axially symmetric Dzyaloshinskii-Moria term¹³

$$DM[m] = \kappa \int_{\mathbb{R}^2} d^2x m \cdot (\nabla \times m). \quad (3.3)$$

Just considering the Dirichlet term, Eq. (3.1), we have the pure $O(3)$ sigma model. A detailed discussion of $O(3)$ sigma model and the lump solutions see [MS04]. In this case finite energy solutions extend to maps $m : S^2 \rightarrow S^2$ and have a well defined topological degree

$$Q[m] = \frac{1}{4\pi} \int d^2x (m \cdot \partial_1 m \times \partial_2 m). \quad (3.4)$$

The energy can be rewritten as

$$E[m] = \frac{1}{2} \int_{\mathbb{R}^2} d^2x (\partial_1 m \pm m \times \partial_2 m)^2 + 2\pi |Q[m]| \geq 2\pi |Q[m]| \quad (3.5)$$

The solutions of the Bogomol'nyi equations,

$$\partial_1 m \pm m \times \partial_2 m = 0, \quad (3.6)$$

saturate the bound and are global minimisers of the energy in a given topological sector.

Exactly what sort of functions solve the Bogomol'nyi equations is most obvious in terms of a stereographic coordinate¹⁴,

$$w = \frac{m_1 + im_2}{1 + m_3}. \quad (3.7)$$

Here the Bogomol'nyi equations become

$$\partial_z w = 0 \quad \text{or} \quad \partial_{\bar{z}} w = 0 \quad (3.8)$$

and are solved in terms of based rational maps, that is rational maps which tend to a constant at infinity.

¹²Sometimes a fourth term, a Lagrange multiplier enforcing the constraint $m^2 = 1$, will be included, $E_{\text{constraint}} = \int_{\mathbb{R}^2} d^2x \lambda (1 - m^2)$. Here we will rarely include the constraint explicitly.

¹³As we shall see later the most general axially symmetric DM term involves a rotated gradient $\nabla_{-\alpha}$ where $\alpha \in [0, 2\pi)$ leading to a family of models. The choice of $\alpha = 0$ (or $\alpha = 2\pi$) is called a Bloch DM term. The unified way of writing this family of models was given in [BSRS20].

¹⁴The inverse stereographic relations are $m_1 + im_2 = \frac{2w}{1+|w|^2}$ and $m_3 = \frac{1-|w|^2}{1+|w|^2}$.

Exercise 3.1. Working in the stereographic coordinates of Eq. (3.7) check that the BPS equations have the form of Eq. (3.8).

Examples of some of these solutions are given in Fig. 5

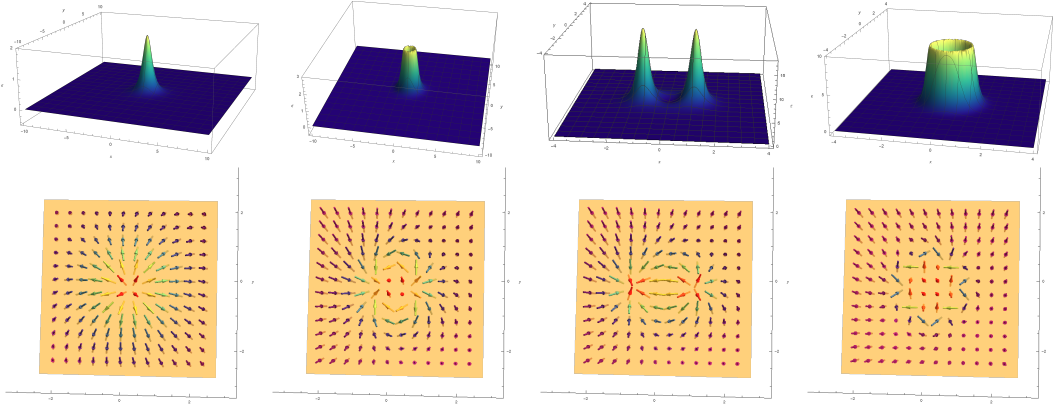


Figure 5: Plots of the energy density and the magnetisation for several choices of rational map. First $w = z$, next $w = z^2$, then $w = (z - 1)(z + 1)$, and finally $w = z^4$. As these are solutions of the Bogomol'nyi equations the energy density is the same as the topological charge density.

Before giving more details we focus briefly on the symmetries of the model. The name $O(3)$ sigma model¹⁵ comes from the $O(3)$ global symmetry of the target S^2 . As stated above for the energy to be finite the field needs to tend to a constant at infinity. The constant can be picked without loss of generality to be

$$\lim_{r \rightarrow \infty} m(r) = e_3 = \begin{pmatrix} 0 \\ 0 \\ 1 \end{pmatrix}. \quad (3.9)$$

This boundary condition breaks the $O(3)$ symmetry down to the $O(2)$ symmetry preserving e_3 . Since the base space has been compactified to $S^2 = \mathbb{R}^2 \cup \{\infty\}$ there are now two $O(2)$ symmetries one for the base and one for the target. These are sometimes referred to as rotations and isorotations respectively¹⁶. Introducing either the potential term, Eq. (3.2), or the DM term, Eq. (3.3), has the potential to break this symmetry further. In fact the DM term is not invariant under rotations and isorotations separately but only the diagonal subgroup. It also breaks the parity symmetry and because of this we refer to the model as chiral¹⁷.

3.2 Derrick's Theorem for chiral magnets

At this point the extra terms that we pal on including, the DM term of Eq. (3.3) and the potential of Eq. (3.2), may make us start to worry about finding non-trivial solutions. In fact

¹⁵The sigma part of the name is because the model is frequently written in terms of the three fields (ϕ_1, ϕ_2, σ) where $\sigma = \sqrt{1 - \phi_1^2 - \phi_2^2}$.

¹⁶The energy functional is also invariant under translations in the plane

¹⁷The version of the DM term with the opposite chirality is $\int_{\mathbb{R}^2} d^2x \bar{m} \cdot (\nabla \times \bar{m})$, where $\bar{m} = (m_1, -m_2, m_3)^T$, which is invariant under the anti-diagonal subgroup [BSRS20].

as we are working in dimension two Derrick's Theorem would suggest that we cannot find any. To see how this is circumvented let us start by considering a scaled version of a static solution $m_\lambda(x, y) \equiv m(\lambda x, \lambda y)$ for $\lambda \in \mathbb{R}_+$. The scaled energy functional is

$$E_\lambda = E_D[m] + \lambda DM[m] + \lambda^2 E_{\text{potential}}, \quad (3.10)$$

with critical points solving

$$\frac{dE_\lambda}{d\lambda} \Big|_{\lambda=1} = -(DM[m] + 2E_{\text{potential}}) = 0. \quad (3.11)$$

Now this equation has solutions when the DM term is negative. This means that adding a term which is not bounded below gives a method of circumventing Derrick's theorem and finding non-trivial solutions to the equations of motion. This is precisely what we turn our attention to now.

Exercise 3.2. Fill in the gaps in the Derrick scaling argument.

3.3 Magnetic Skyrmions model

The theoretical model of magnetic skyrmions were first introduced by Bogdanov and collaborators in [BH94, BY89]. Experimental and theoretical studies of magnetic skyrmions are reviewed in [NT13].

3.3.1 The vacuum manifold

Moving now to considering chiral magnets we include the DM term and potential, Eqs. (3.2) and (3.3) in the energy. As part of this we specify the type of potential term that we work with and explore the structure of its vacuum manifold \mathcal{V} . As we are considering a magnetic material the first kind of term that can appear in the potential is a Zeeman term measuring the response of m to an external magnetic field \vec{B} , conventionally we align the external field with the 3-axis and take

$$\vec{B} = \begin{pmatrix} 0 \\ 0 \\ B \end{pmatrix}. \quad (3.12)$$

The Zeeman term¹⁸ is thus

$$U_Z(m) = -B m_3, \quad (3.13)$$

this term is minimised when m is aligned with \vec{B} , in this case when

$$m_3 = \begin{pmatrix} 0 \\ 0 \\ \frac{B}{|B|} \end{pmatrix}. \quad (3.14)$$

¹⁸A more general Zeeman term is $\vec{B} \cdot m$. We are interested in a two dimensional model with everything independent of the third direction. This makes it convenient to align the magnetic field with the symmetry axis of the material.

The next type of term that can appear in the potential is an anisotropy term which describes an asymmetry in the model. We are interested in the case of anisotropy in the third direction and the corresponding term in the potential is

$$U_A(m) = A m_3^2. \quad (3.15)$$

Depending on the sign of A this leads to different minima: When A is positive the potential is minimised by $m_3 = 0$, so the magnetisation lies in the x-y plane and the anisotropy is referred to as being easy plane. When A is negative Eq. (3.15) is minimised by $m_3 = \pm 1$ and the anisotropy is referred to as being easy axis.

Putting all of this together the energy functional is

$$E[m] = \int_{\mathbb{R}^2} d^2x \left[\frac{1}{2} (\nabla m)^2 + \kappa m \cdot (\nabla \times m) + A m_3^2 - B m_3 \right]. \quad (3.16)$$

This energy functional is invariant under $B \rightarrow -B$, $m \rightarrow -m$ so we can restrict our attention to $B \geq 0$. Finally it is convenient to add $B - A$ as a constant to the potential so that the energy functional takes the form

$$E[m] = \int_{\mathbb{R}^2} d^2x \left[\frac{1}{2} (\nabla m)^2 + \kappa m \cdot (\nabla \times m) - A (1 - m_3^2) + B (1 - m_3) \right]. \quad (3.17)$$

The vacuum manifold is given

$$\mathcal{V} = \{m \mid -A (1 - m_3^2) + B (1 - m_3) = 0\}, \quad (3.18)$$

Depending on the values of A and B this takes different forms. When $B > 2A$ it is the single point $\mathcal{V}_{B>2A} = \{m = e_3\}$ and when $B < 2A$ it is the circle

$$\mathcal{V}_{B<2A} = \left\{ m_3 = \frac{B}{2A}, (m_1)^2 + (m_2)^2 = 1 - \frac{B^2}{4A^2} \right\} \simeq S^1. \quad (3.19)$$

How the vacuum manifolds relate to the target S^2 are plotted in Fig. 6.

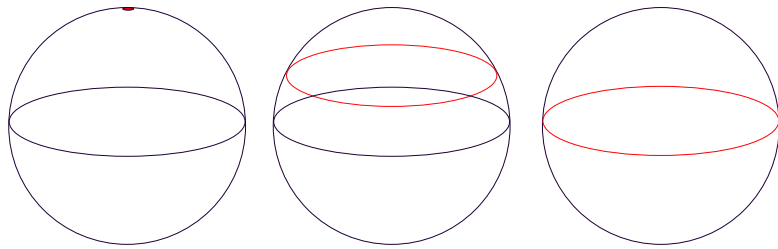


Figure 6: Plots of the vacuum manifold in red on the target S^2 . On the left is $B > 2A$ with the vacuum manifold $\mathcal{V}_{B>2A} = \{m = e_3\}$, in the middle is $B < 2A$ with $\mathcal{V}_{B<2A} = \left\{ m_3 = \frac{B}{2A}, (m_1)^2 + (m_2)^2 = 1 - \frac{B^2}{4A^2} \right\}$, and on the right is $B = 0$ with $\mathcal{V}_{B=0} = \{m_3 = 0, (m_1)^2 + (m_2)^2 = 1\}$ the circle at the equator.

Exercise 3.3. By minimising the potential check that these are the vacuum manifolds that you find.

3.3.2 Hedgehogs and symmetries of the model

Before discussing one approach to constructing skyrmion solutions it is convenient to mention the symmetries of the model in Eq. (3.17). It is invariant under translations in the $x - y$ -plane and under the $O(2)$ subgroup which acts through rotations and reflections as

$$m(x, y) \mapsto R(\sigma)m(\cos \sigma x - \sin \sigma y, \sin \sigma x + \cos \sigma y), \quad \sigma \in [0, 2\pi), \quad (3.20)$$

$$m(x, y) \mapsto R(2\gamma)\bar{m}(x, -y), \quad \text{with } \gamma = \frac{\pi}{2} - \alpha, \quad (3.21)$$

with $R(\sigma)$ a rotation about the third direction given by

$$R(\sigma) = \begin{pmatrix} \cos \sigma & \sin \sigma & 0 \\ \sin \sigma & \cos \sigma & 0 \\ 0 & 0 & 1 \end{pmatrix} \quad (3.22)$$

and

$$\bar{m} = \begin{pmatrix} m_1 \\ -m_2 \\ m_3 \end{pmatrix}. \quad (3.23)$$

This is the group of rotations and reflections in the $x - y$ plane combined with simultaneous rotation and reflection of the target sphere. For nuclear and baby skyrmions the rotations and reflections of the target space are called isorotations and isoreflections. It is the DM term which breaks the product group $O(2) \times O(2)$ down to the diagonal subgroup.

When looking for solutions it is convenient to write the magnetisation in terms of spherical polar coordinates as

$$m = \begin{pmatrix} \sin \Theta \cos \Phi \\ \sin \Theta \sin \Phi \\ \cos \Theta \end{pmatrix} \quad (3.24)$$

with Θ and Φ functions on the plane. Such a solution is invariant under the $O(2)$ symmetry group of the model when $\Theta = \Theta(r)$ and $\Phi = \varphi + \gamma$ with (r, φ) the plane polar coordinates and $\gamma = \frac{\pi}{2} - \alpha$. Such an expression is called a hedgehog field¹⁹. Taking the boundary conditions that

$$\Theta(0) = \pi, \quad \text{and } \Theta(\infty) = 0, \quad (3.25)$$

gives a hedgehog field with $Q = -1$.

Exercise 3.4. Using Eq. (3.4) compute the degree of a hedgehog field configuration satisfying the boundary conditions in Eq. (3.25).

Assuming that the fields tend to \mathcal{V} as $\vec{x} \rightarrow \infty$ enables us to add the point at infinity and work with the domain $\mathbb{R}^2 \cup \{\infty\} = S^2$. For the $O(3)$ sigma model this condition ensures finite energy of the solutions. This means that field configurations will be maps $m : S^2 \rightarrow S^2$ with

¹⁹Taking $\Phi = n\varphi + \gamma$ would lead to a configuration with $Q = -n$. However, these are unstable configurations [FKA⁺19]

a well defined topological degree given by Eq. (3.4). When we discuss the critically coupled model we will encounter some skyrmion configurations for which m does not extend to a map between spheres. For these configurations the integral in Eq. (3.4) will not have its topological interpretation. However, it can still be evaluated and is found to still be an integer. One way to avoid this complication is to redefine the energy functional to remove a boundary term. We will comment on this more thoroughly in a later section as there are analytic reasons to make this redefinition.

For hedgehog fields the energy functional becomes

$$E = 2\pi \int_0^\infty r dr \left(\frac{1}{2} \left(\frac{d\Theta}{dr} \right)^2 + \frac{\sin^2 \Theta}{2r^2} + \kappa \left(\frac{d\Theta}{dr} + \frac{\sin(2\Theta)}{2r} \right) + B(1 - \cos \Theta) - A(1 - \cos^2 \Theta) \right) \quad (3.26)$$

with the equation of motion

$$\frac{d^2\Theta}{dr^2} = -\frac{1}{r} \frac{d\Theta}{dr} + \frac{\sin(2\Theta)}{2r^2} - 2\kappa \frac{\sin^2 \Theta}{r} + B \sin \Theta - A \sin(2\Theta). \quad (3.27)$$

In the region $B \geq 2A$ this can be solved numerically to find $Q = -1$ configurations. Examples of some of these numerical solutions, including non reflection invariant conditions with $\gamma \neq \frac{\pi}{2} - \alpha$, are given in [FKA⁺19] and three examples are plotted below in Fig. 9. Depending on the specifics of the DM term, the value of α , the skyrmions are either of Bloch or Néel type. A schematic of the magnetisation vector field of a skyrmion is given in Fig. 7.

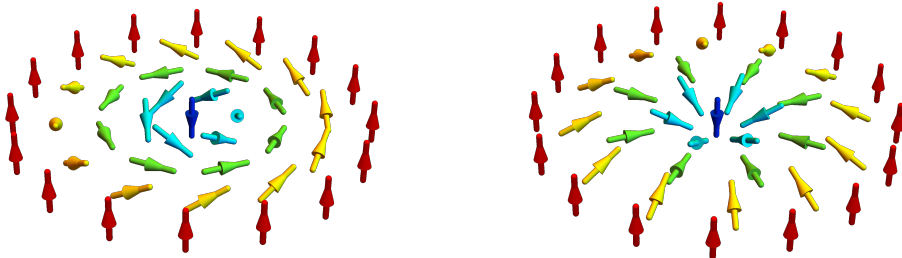


Figure 7: Illustrative Mathematica plots of the axially-symmetric Bloch and Néel skyrmion.

3.4 The solvable line

In the $O(3)$ sigma model we were able to explicitly construct solutions by finding and solving first order Bogomol'nyi equations. It turns out that something similar can be done for the more general model in Eq. (3.17) when $B = 2A$. To describe this in detail we start by assuming the magnetisation takes the form of the hedgehog ansatz in Eq. (3.24). The equation of motion,

Eq. (3.27), becomes

$$\frac{d^2\Theta}{dr^2} = -\frac{1}{r} \frac{d\Theta}{dr} + \frac{\sin(2\Theta)}{2r^2} - 2\kappa \frac{\sin^2\Theta}{r} + B \sin\Theta (1 - \cos\Theta). \quad (3.28)$$

Written in terms of the hedgehog ansatz the $O(3)$ Bogomol'nyi equations, Eq. (3.6), are

$$\frac{d\Theta}{dr} + \frac{\sin\Theta}{r} = 0, \quad (3.29)$$

which is solved, along with the boundary conditions from Eq. (3.25), by

$$\Theta = 2 \arctan\left(\frac{2}{\lambda r}\right), \quad \lambda \in \mathbb{R}. \quad (3.30)$$

Taking the r derivative of Eq. (3.29) gives

$$\frac{d^2\Theta}{dr^2} = -\frac{1}{r} \frac{d\Theta}{dr} + \frac{\sin(2\Theta)}{2r^2}. \quad (3.31)$$

This is nothing but the first three terms from the equation of motion, Eq. (3.28). Thus we find that the profile function in Eq. (3.30) will solve the equations of motion for $\lambda = \frac{B}{\kappa}$.

Exercise 3.5. Show that the hedgehog profile function, Eq. (3.29) solves the equations of motion Eq. (3.28).

Examples of these hedgehog configurations are given in Fig. 8.

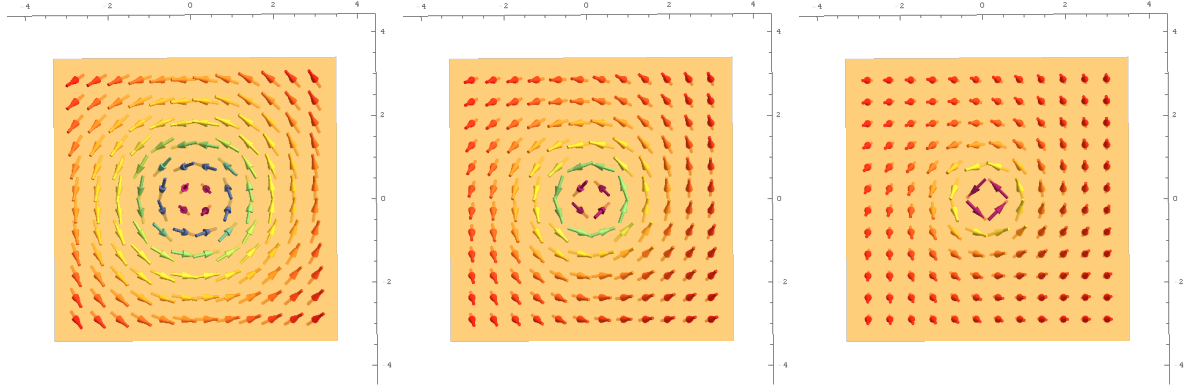


Figure 8: Mathematica plots of the hedgehog configurations for $B = \kappa^2$, $B = 2\kappa^2$, and $B = 4\kappa^2$. These are all plots of the Bloch configurations with $\alpha = 0$ and $\gamma = \frac{\pi}{2}$. The size of the skyrmion is decreasing with increasing B .

At the level of the energy functional the DM and potential terms cancel point wise

$$m^B \cdot (\nabla \times m^B) = \frac{B}{2} (1 - m_3^B)^2, \quad (3.32)$$

where m^B is the hedgehog configuration corresponding to the profile function

$$\Theta = 2 \arctan \left(\frac{2\kappa}{Br} \right). \quad (3.33)$$

The energy is thus given purely by the Dirichlet term, Eq. (3.1), which satisfies the Bogomol'nyi energy bound, Eq. (3.5). The hedgehog configurations then have energy

$$E[m^B] = 4\pi. \quad (3.34)$$

For the topological solitons that we encountered in the previous section, ϕ^4 and sine-Gordon kinks, there is an infinite energy barrier protecting the skyrmion from decaying to the vacuum. For magnetic skyrmions this is not the case, by changing γ we can find skyrmion configurations with energy 4π and zero size, see Fig. 9. Thus the energy barrier is finite in this case! This causes some people to refer to magnetic skyrmions as “non topological” solitons.

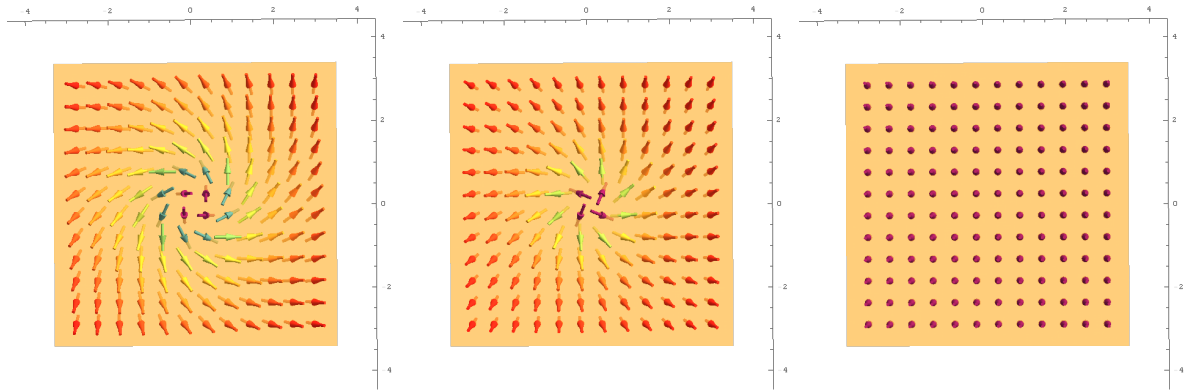


Figure 9: Mathematica plots of the hedgehog configurations for $B = \kappa^2$, $\alpha = 0$ and varying γ . The size of the skyrmion is decreasing with decreasing γ . On the left $\gamma = \frac{\pi}{4}$, in the middle $\gamma = \frac{\pi}{8}$, and on the right $\gamma = 0$.

3.5 The critically coupled model

Specialising the model even more results in a gauged version of the $O(3)$ sigma model that we met earlier. The key observation to realise this is that a term in the energy which is first order in derivatives can be reinterpreted as a gauge field. This means that there are a lot of similarities between magnetic skyrmions and sigma model lumps. Spelling this out is what we now turn to. The critically coupled model was first introduced in [BSRS20] and involves fine tuning the potential to be $B = \kappa^2$. The energy functional for the critically coupled model is

$$E_{cc}[m] = \int_{\mathbb{R}^2} d^2x \left[\frac{1}{2} |\nabla m|^2 + \kappa m \cdot (\nabla_{-\alpha} \times m) + \frac{\kappa^2}{2} (1 - m_3)^2 \right] \quad (3.35)$$

Introducing the covariant derivative, also known as the helical derivative,

$$D_i m = \partial_i m - \kappa e_i \times m, \quad (3.36)$$

with the gauge potential and field strength being

$$A_i = -i\kappa e_i, \quad (3.37)$$

$$F_{12} = \kappa^2 e_3, \quad (3.38)$$

leads to a convenient rewriting of the model. Two useful identities, the second of which was first observed in [Hoo74], are

$$(D_1 m + m \times D_2 m)^2 = (D_1 m)^2 + (D_2 m)^2 - 2(D_1 m \times D_2 m) \cdot m, \quad (3.39)$$

$$(D_1 m \times D_2 m) \cdot m - m \cdot F_{12} = (\partial_1 m \times \partial_2 m) \cdot m + \partial_2(m \cdot A_1) - \partial_1(m \cdot A_2). \quad (3.40)$$

Making use of these we have the following result about the critically coupled model [BSRS20].

Lemma 3.6. *The energy of the critically coupled model can be written as*

$$E[m] = 4\pi(Q[m] + \Omega[m]) + \int d^2x (D_1 m + m \times D_2 m)^2, \quad (3.41)$$

where $\Omega[m]$, called the total vortex strength, is

$$\Omega[m] = \frac{\kappa}{4\pi} \int d^2x e_3 \cdot (\nabla_{-\alpha} m \times m) \quad (3.42)$$

Equality holds if and only if the Bogomol'nyi equations

$$D_1 m + m \times D_2 m = 0 \quad (3.43)$$

is satisfied.

The vortex strength term gets its name because $e_3 \cdot (\nabla_{-\alpha} m \times m)$ is the vorticity of the first two components, m_1, m_2 . Stokes' theorem tells us that it is a boundary term, as

$$e_3 \cdot (\nabla_{-\alpha} m \times m) dx \wedge dy = \kappa d(m_1^\alpha dx + m_2^\alpha dy). \quad (3.44)$$

There are some problematic configurations for which $\Omega[m]$ is not defined and it is necessary to regularise it as

$$\Omega^\circ[m] = \frac{1}{4\pi} \lim_{R \rightarrow \infty} \int_{C_R} \kappa d(m_1^\alpha dx + m_2^\alpha dy), \quad (3.45)$$

with C_R the circle of radius R . As we will comment on later the boundary term issues can be circumvented by starting from a modified energy functional where the boundary piece has been subtracted off. This modified setting is discussed in detail in [Sch19a, Sch19b], in [Wal20] the combination $Q[m] + \Omega[m]$ was interpreted as the equivariant degree of m . Here we are most interested in showcasing some of the interesting configurations so we put off discussion of the boundary term.

The proof of the result is by direct computation and filling in the details is left as an exercise for the reader.

One of the key differences between this gauged model and the ordinary, ungauged, $O(3)$ sigma model is that the energy bound is in terms of the degree $Q[m]$ rather than the modulus of the

degree. When we meet the solutions of the Bogomol'nyi equations we will see that the lowest degree solution is the $Q = -1$ skyrmion with energy 4π and that all other solutions have higher Q .

As in the case of the $O(3)$ sigma model the easiest way to understand the solutions is to use complex stereographic coordinates of Eq. (3.7), in particular the inverse coordinates $v = \frac{1}{w}$. In these coordinates the degree and total vortex strength become

$$Q[w] = \frac{i}{2\pi} \int d^2x \frac{\partial_1 w \partial_2 \bar{w} - \partial_2 w \partial_1 \bar{w}}{(1 + |w|^2)^2}, \quad (3.46)$$

$$\Omega[w] = \frac{\kappa}{\pi} \int d^2x \operatorname{Im} \left(e^{i\alpha} \frac{\partial_z w - w^2 \partial_z \bar{w}}{(1 + |w|^2)^2} \right). \quad (3.47)$$

The energy bound is then

$$E[w] = 4\pi (Q[w] + \Omega[w]) + 8 \int d^2x \frac{|\partial_{\bar{z}} w - \frac{i}{2}\kappa e^{i\alpha} w^2|^2}{(1 + |w|^2)^2}, \quad (3.48)$$

with the Bogomol'nyi equations written in terms of $v = \frac{1}{w}$ as

$$\partial_{\bar{z}} v = -\frac{i}{2}\kappa e^{i\alpha}. \quad (3.49)$$

The general solution to these Bogomol'nyi equations is given by

$$v = -\frac{i}{2}\kappa e^{i\alpha} \bar{z} + f(z), \quad (3.50)$$

with f an arbitrary holomorphic function.

For $f(z) = \frac{p(z)}{q(z)}$ with p and q polynomials in z of degree m and n with no common factors, we can prove a nice result about the energy.

Lemma 3.7. *For a skyrmion configuration given by*

$$v = -\frac{i}{2}\kappa e^{i\alpha} \bar{z} + \frac{p(z)}{q(z)}, \quad (3.51)$$

with p and q polynomials of degree m and n respectively, the integral defining the total energy is well defined provided $m \neq n + 1$. The energy is

$$E[w] = 4\pi \max(m, n + 1) \quad \text{if } m \neq n + 1. \quad (3.52)$$

When $m = n + 1$ the total energy is not well defined but the regularised total energy is

$$E[w] = 4\pi (Q[w] + \Omega^0[w]) = 4\pi m \quad (3.53)$$

Rational configurations are our main focus so we set

$$N = \max(m, n + 1). \quad (3.54)$$

For interested readers the proof of this result is in [BSRS20].

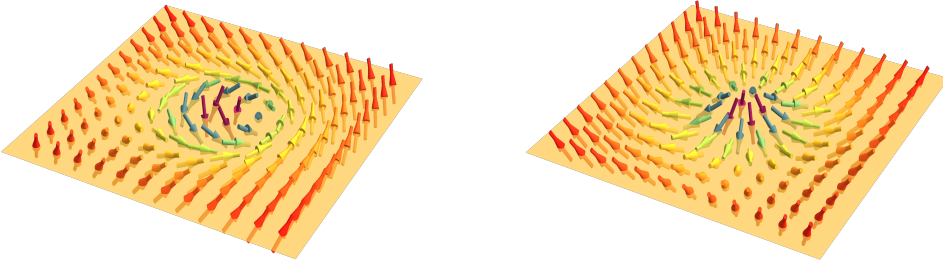


Figure 10: Left to right: Magnetisation plot of a Bloch skyrmion and a Néel skyrmion.

3.5.1 A zoo of skyrmions

There are many easy to construct examples of solutions to the Bogomol'nyi equations. In this section we showcase this zoo of skyrmion anti-skyrmion configurations starting with the $E = 4\pi$ sector and going up in multiples of 4π .

N=1 There is a four dimensional family of solutions

$$v_1 = -\frac{i}{2}\kappa e^{i\alpha}(\bar{z} + az) + b, a, b \in \mathbb{C}. \quad (3.55)$$

Translations and rotations fix everything except from $|a|$. Changing $|a|$ corresponds to a stretching or squeezing of the energy density. The simplest example is $a = b = 0$, with $\alpha = 0$ this is called the Bloch skyrmion and with $\alpha = \frac{\pi}{2}$ this is a Néel skyrmion. These are plotted in Fig. 10.

The stretching and squeezing effect is shown in Fig. 11. Keeping $|a|$ fixed and changing the phase of a leads to rotations of the energy density. As shown in Fig 12 the energy density rotates by half the angle that a changes by.

Another interesting feature is that changing $|a|$ changes the degree. When $|a| > \frac{1}{2}$, $Q = 1$ and the solutions is an anti-skyrmions as shown in Fig. 13. This means that by increasing $|a|$ through the problematic value of $|a| = \frac{1}{2}$ a skyrmion can be turned in to and anti-skyrmion.

Within the family of solutions with regularised energy 4π configurations with $|a| = \frac{1}{2}$, such as

$$v = -\frac{i}{2}e^{i\alpha}(\bar{z} + e^{i\delta}z) \quad (3.56)$$

are particularly interesting. These solutions have a whole line where $m_3 = -1$, $\varphi = -\frac{\delta}{2} \pm \pi$, and are examples of solutions which do not extend to maps of spheres.

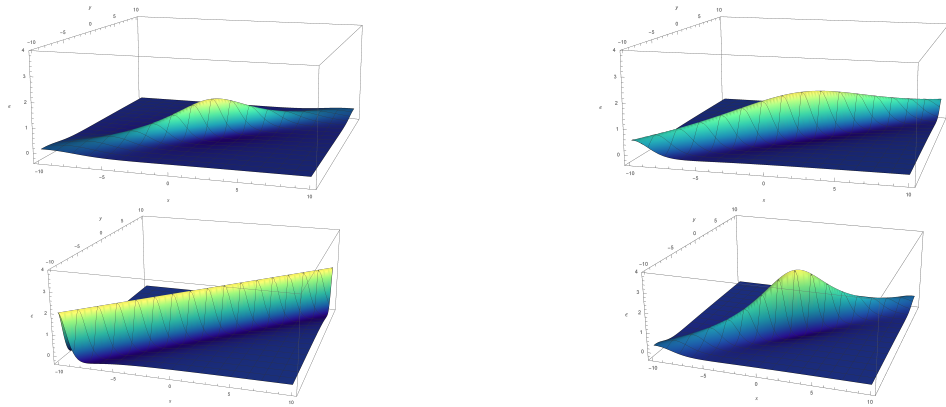


Figure 11: Stretching and squeezing for the configuration $v = -\frac{i}{2}\bar{z} + az$ with $a = 0.3$ (top left), $a = 0.4$ (top right), $a = 0.5$ (bottom left) and $a = 0.7$ (bottom right).

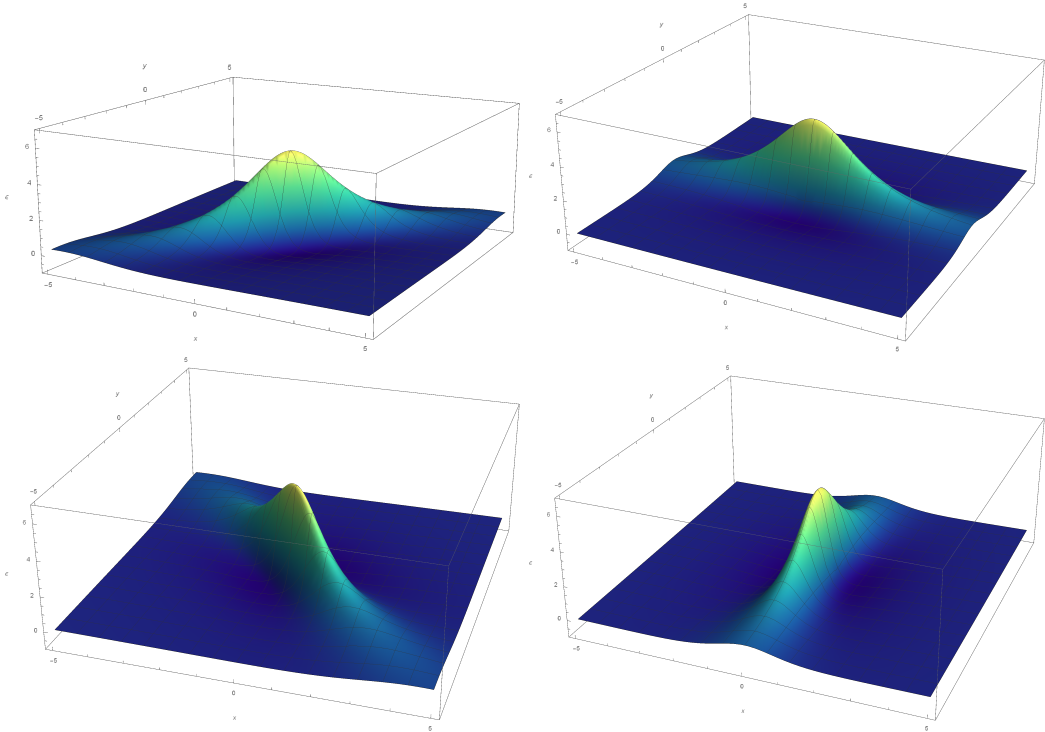


Figure 12: Rotation of the energy density of $v = -\frac{i}{2}\bar{z} + az$ when $|a| > \frac{1}{2}$: $a = 1$ (top left), $a = e^{i\pi/2}$ (top right), $a = e^{i\pi}$ (bottom left) and $a = e^{i3\pi/2}$ (bottom right).

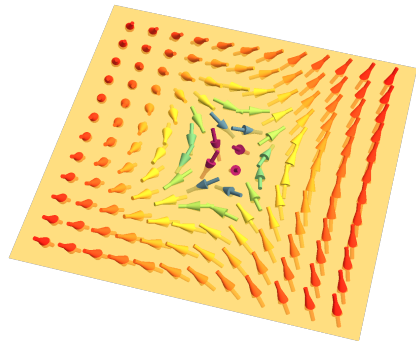


Figure 13: For $v = -\frac{i}{2}\bar{z} + 3iz$ the magnetisation rotates oppositely to that of the Bloch skyrmion.

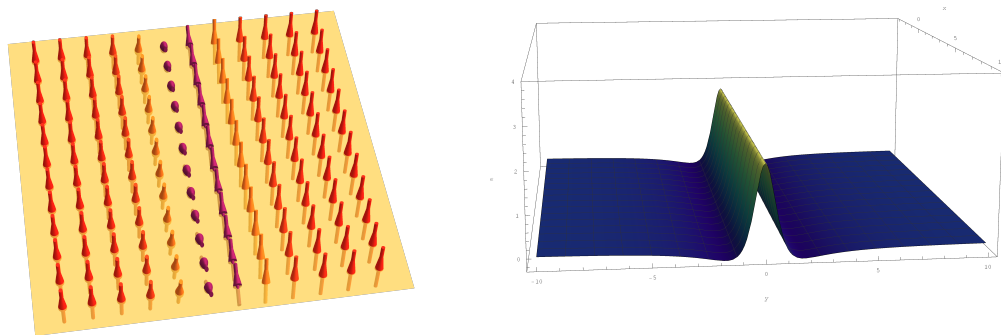


Figure 14: Left to right: magnetisation plot and energy density plot for the solution $v = -\frac{i}{2}(\bar{z} - z)$

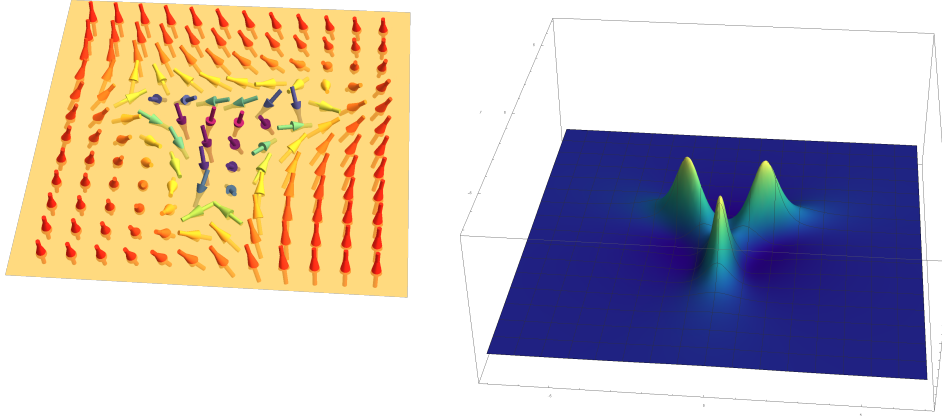


Figure 15: Magnetisation and energy density for $v = -\frac{i}{2}\bar{z} + \frac{1}{2}z^2$. This is an example of a configuration involving a skyrmion and three anti-skyrmions.

For these configurations the energy density is peaked long the line as shown in Fig. 14. These configurations are lost if we work with the modified energy of [Sch19b, Sch19a] and are one of the reasons we need to work with the regularised energy.

N=2 Moving to the next energy sector there is an eight dimensional family of solutions

$$v = -\frac{i}{2}\kappa e^{i\alpha}\bar{z} + \frac{az^2 + bz + c}{dz + e}, \quad (3.57)$$

with $a, b, c, d, e \in \mathbb{C}$, and $(a, b, c, d, e) \sim \lambda(a, b, c, d, e)$, $\lambda \in \mathbb{C}^*$.

In this family we find solutions which are a combination of skyrmions and anti-skyrmions. Examples of some of these solutions are in Figs. 15 and 16

An interesting feature that arises at $E = 8\pi$ are the $Q = 0$ skyrmion bags or sacks, which have been seen numerically in the full model by [FKA⁺19, RK19]. In the critically coupled model these configurations arise when

$$v = -\frac{i}{2}\kappa e^{i\alpha} \left(\bar{z} - \frac{R^2}{z} \right) \quad \text{with } R \in \mathbb{R}_{>0}. \quad (3.58)$$

Plotting the magnetisation vector field of these configurations show that they have a circle of south poles at R , the radius of the bag, with vacuum, $m = e_3$ in the centre. These bags are some of the most symmetric solutions as, like the basic holomorphic solution, they are invariant under spin-isospin rotations. An example of a bag configuration is given in Fig. 17. As these configurations have $Q = 0$ they are non-topological soliton configurations, even when the alternative energy functional is used.

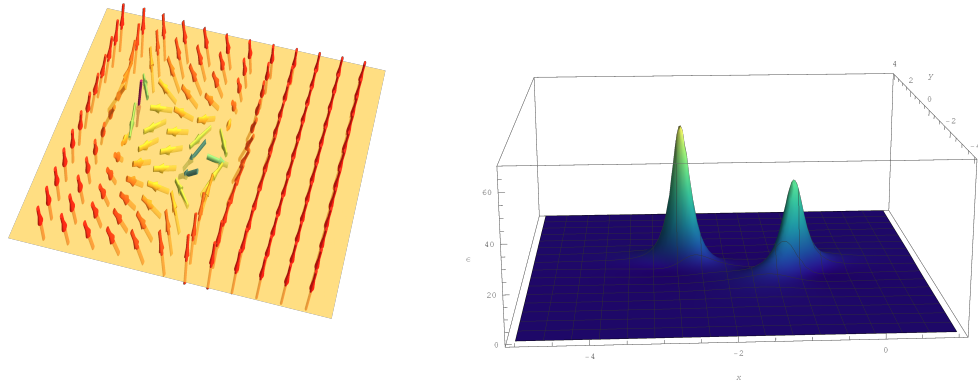


Figure 16: Magnetisation and energy density for $v = -\frac{i}{2}\bar{z} + 2z^2 + 7z + 5$. There are two anti-skyrmions.

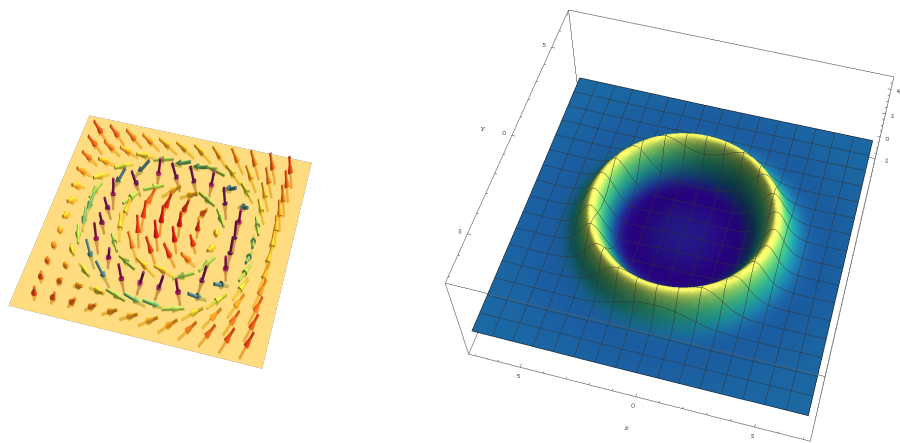


Figure 17: Magnetisation and energy density for the skyrmion bag defined by $v = -\frac{i}{2}(\bar{z} - \frac{16}{z})$.

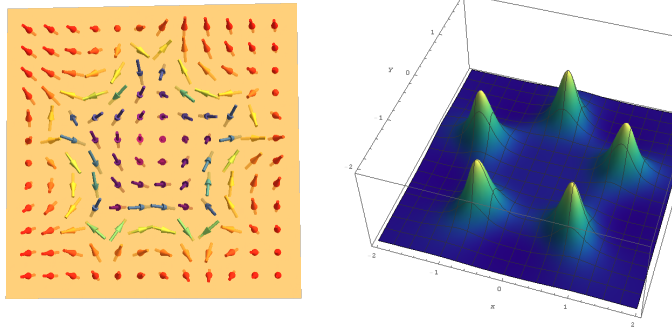


Figure 18: Magnetisation and energy density for $v = -\frac{i}{2}\bar{z} + \frac{1}{2}z^4$. There are five anti-skyrmions surrounding one skyrmion at the centre.

The higher energy solutions have been less studied but we can find solutions with interesting configurations arising. In fact configurations of the form

$$v = -\frac{i}{2}e^{i\alpha} \left(\bar{z} - \frac{z^n}{R^{n-1}} \right), \quad R \in \mathbb{R}_{>0}, n \in \mathbb{Z}_{>1}, \quad (3.59)$$

have degree n and $n+2$ zeros: one at the origin and $n+1$ at

$$z_k = Re^{\frac{2\pi ki}{n+1}}, \quad k = 0, \dots, n. \quad (3.60)$$

The zero at the origin corresponds to a $Q = -1$ skyrmion while the $n+1$ zeros correspond to $Q = 1$ anti-skyrmions. An example of a degree four configuration is given in Fig. 18.

The question of computing the number of zeros of expressions like Eq. (3.51) is hard to answer as the number of zeros can exceed the absolute value of the degree, as we see in our examples. See [KN04, BHJR13, FKK07] for more details about degrees and zeros of harmonic functions.

3.6 A comment on boundary terms

One of the unexpected features of the magnetic skyrmion model is the subtlety associated with boundary contributions to the energy. This was first noted in [DM16] where it was observed that the variational problem for the DM term is not well defined as currently stated. It was also commented on in the final version of [BSRS20] as well as being one of the subjects of study in [Sch19a, Sch19b]. The boundary term is important for the solvable line as here there are configurations which fall off as $\frac{1}{r}$. However, for $B > 2A$ it can be shown that configurations fall off exponentially so the boundary term is zero in this case. Varying the DM term, Eq. (3.3), with respect to m we find

$$DM[m + \delta m] = \kappa \int_{\mathbb{R}^2} d^2x [m \cdot (\nabla \times m) + 2\delta m \cdot (\nabla \times m) - \nabla \cdot (m \times \delta m) + \mathcal{O}(\delta m^2)], \quad (3.61)$$

$$= DM[m] + \kappa \int_{\mathbb{R}^2} d^2x [2\delta m \cdot (\nabla \times m) - \nabla \cdot (m \times \delta m) + \mathcal{O}(\delta m^2)]. \quad (3.62)$$

The first term of order δn is the one that contributes to the equation of motion, while the second term is a boundary term. Typically the conditions $\lim m \rightarrow m_\infty \in \mathcal{V}$ and $\lim \delta m \rightarrow 0$ are enough to ensure that the boundary term vanishes, however, when the fields can fall off as $\frac{1}{r}$ this is no longer enough. The issue can be rectified by subtracting the boundary term

$$\text{BT}[m] = -\kappa \int_{\mathbb{R}^2} d^2x \nabla \cdot (m_\infty \times m), \quad (3.63)$$

when m_∞ is constant, as it is for $B \geq 2A$, this can be simplified to

$$\text{BT}[m] = -\kappa \int_{\mathbb{R}^2} d^2x m_\infty \cdot (\nabla \times m) = 4\pi\Omega[m]. \quad (3.64)$$

Subtracting this boundary term for the critically coupled model the energy bound is now purely in terms of the topological degree. This now means that the skyrmion and anti-skyrmion, $f = 0$ and $f = az$, configurations have different energy.

3.7 A view to the future

The critically coupled model of magnetic skyrmions which we encountered here is just one example of a family of models which describe topological solitons in magnetic systems. The gauged sigma model interpretation was generalised in [Sch19b] to describe a wider range of models. To sketch the general story for a gauged sigma model there is a Bogomol'nyi bound in terms of the topological degree, upto a boundary term. These Bogomol'nyi equations can be solved in terms of a $SL(2, \mathbb{C})$ valued function. Specifying the connection reduces this general model to particular case. For example picking an “axially-symmetric” connection²⁰ leads to the critically coupled model we have studied here. Different choices of connection correspond to different systems. For a full explanation of this generalisation the interested reader is referred to [Sch19b].

Acknowledgements First and foremost I want to thank Bernd Schroers who was my PhD supervisor for introducing me to the wonderful world of solitons. I also want to thank Benoit Vicedo for organising these lectures and giving me the opportunity to give two of them. Finally I want to thank Benoit Vicedo, Bernd Schroers, Bruno Barton-Singer, Grigoris Giotopoulos and Lukas Müller for reading through these notes and offering comments and corrections.

References

- [BH94] A. Bogdanov and A. Hubert. Thermodynamically stable magnetic vortex states in magnetic crystals. *Journal of Magnetism and Magnetic Materials*, 138(3):255 – 269, 1994.
- [BHJR13] Pavel M. Bleher, Youkow Homma, Lyndon L. Ji, and Roland K. W. Roeder. Counting Zeros of Harmonic Rational Functions and its Application to Gravitational Lensing. *International Mathematics Research Notices*, 2014(8):2245–2264, 01 2013.

²⁰The quotes are because what we pick is an axially-symmetric DM term and this puts constraints on the connection.

- [BSRS20] Bruno Barton-Singer, Calum Ross, and Bernd J. Schroers. Magnetic Skyrmions at Critical Coupling. *Commun. Math. Phys.*, 2020.
- [BY89] A. Bogdanov and D. A. Yablonskii. Thermodynamically stable vortices in magnetically ordered crystals. the mixed state of magnets. *Zh. Eksp. Teor. Fiz.*, 95:178 – 182, 1989.
- [Col88] Sidney Coleman. *Aspects of Symmetry: Selected Erice Lectures*. Cambridge University Press, 1988.
- [Der64] G. H. Derrick. Comments on nonlinear wave equations as models for elementary particles. *Journal of Mathematical Physics*, 5(9):1252–1254, 1964.
- [DM16] Lukas Döring and C. Melcher. Compactness results for static and dynamic chiral skyrmions near the conformal limit. *Calculus of Variations and Partial Differential Equations*, 56:60, 2016.
- [Dun10] M. Dunajski. *Solitons, Instantons, and Twistors*. Oxford Graduate Texts in Mathematics. OUP Oxford, 2010.
- [FKA⁺19] David Foster, Charles Kind, Paul J. Ackerman, Jung-Shen B. Tai, Mark R. Dennis, and Ivan I. Smalyukh. Two-dimensional skyrmion bags in liquid crystals and ferromagnets. *Nature Phys.*, 15(7):655–659, 2019.
- [FKK07] C. D. Fassnacht, C. R. Keeton, and D. Khavinson. Gravitational lensing by Elliptical Galaxies, and the Schwarz Function. *arXiv e-prints*, page arXiv:0708.2684, August 2007.
- [Hat00] Allen Hatcher. *Algebraic topology*. Cambridge Univ. Press, Cambridge, 2000.
- [Hoo74] G.’t Hooft. Magnetic monopoles in unified gauge theories. *Nuclear Physics B*, 79(2):276 – 284, 1974.
- [KN04] Dmitry Khavinson and Genevra Neumann. On the number of zeros of certain rational harmonic functions. *arXiv Mathematics e-prints*, page math/0401188, January 2004.
- [MF53] P.M.C. Morse and H. Feshbach. *Methods of Theoretical Physics, I*. International series in pure and applied physics. McGraw-Hill, 1953.
- [MS04] N. S. Manton and P. M. Sutcliffe. *Topological solitons*. Cambridge monographs on mathematical physics. Cambridge University Press, Cambridge, July 2004.
- [NT13] Naoto Nagaosa and Yoshinori Tokura. Topological properties and dynamics of magnetic skyrmions. *Nature nanotechnology*, 8 12:899–911, 2013.
- [RK19] Filipp N. Rybakov and Nikolai S. Kiselev. Chiral magnetic skyrmions with arbitrary topological charge. *Phys. Rev. B*, 99:064437, Feb 2019.
- [Sch19a] Bernd Schroers. Solvable Models for Magnetic Skyrmions. In *11th International Symposium on Quantum Theory and Symmetries (QTS2019) Montreal, Canada, July 1-5, 2019*, 2019.

- [Sch19b] Bernd J. Schroers. Gauged Sigma Models and Magnetic Skyrmions. *SciPost Phys.*, 7(3):030, 2019.
- [Wal20] Edward Walton. On the geometry of magnetic skyrmions on thin films. *Journal of Geometry and Physics*, 156:103802, 2020.